

Variability of ozone in the marine boundary layer of the equatorial Pacific Ocean

Xiao-Ming Hu · Jeffrey M. Sigler · Jose D. Fuentes

Received: 29 December 2010 / Accepted: 26 July 2011
© Springer Science+Business Media B.V. 2011

Abstract This study examines the processes controlling the diurnal variability of ozone (O_3) in the marine boundary layer of the Kwajalein Atoll, Republic of the Marshall Islands (latitude $8^\circ 43' N$, longitude $167^\circ 44' E$), during July to September 1999. At the study site, situated in the equatorial Pacific Ocean, O_3 mixing ratios remained low, with an overall average of 9–10 parts per billion on a volume basis (ppbv) and a standard deviation of 2.5 ppbv. In the absence of convective storms, daily O_3 mixing ratios decreased after sunrise and reached minimum during the afternoon in response to photochemical reactions. The peak-to-peak amplitude of O_3 diurnal variation was approximately 1–3 ppbv. During the daytime, O_3 photolysis, hydroperoxyl radicals, hydroxyl radicals, and bromine atoms contributed to the destruction of O_3 , which explained the observed minimum O_3 levels observed in the afternoon. The entrainment of O_3 -richer air from the free troposphere to the local marine boundary layer provided a recovery mechanism of surface O_3 mixing ratio with a transport rate of 0.04 to 0.2 ppbv per hour during nighttime. In the presence of convection, downward transport of O_3 -richer tropospheric air increased surface O_3 mixing ratios by 3–12 ppbv. The magnitude of O_3 increase due to moist convection was lower than that observed over the continent (as high as 20–30 ppbv). Differences were ascribed to the higher O_3 levels in the continental troposphere and weaker convection over the ocean. Present results suggest that moist convection plays a role in surface-level O_3 dynamics in the tropical marine boundary layer.

Keywords Ozone · Marine boundary layer · Tropical meteorology · Deep convection

X.-M. Hu · J. D. Fuentes (✉)
Department of Meteorology, Pennsylvania State University, University Park, PA 16802, USA
e-mail: jdfuentes@psu.edu

J. M. Sigler
Department of Environmental Sciences, Tulane University, New Orleans, LA, USA

1 Introduction

Ozone (O_3) is an important constituent in the Earth's troposphere due to its role as a greenhouse gas, secondary pollutant, and contribution to influencing atmospheric chemical cycles. In the moist atmospheric boundary layer O_3 is an important precursor of the hydroxyl radical (OH) which drives a plethora of atmospheric chemical cycles. Hydroxyl radicals are formed when O_3 undergoes photolysis to produce atomic oxygen in the electronically excited state ($O(^1D)$) that readily combines with water vapor to produce OH. While O_3 sinks and sources are relatively well established in the continental boundary layer (CBL), the processes that drive O_3 dynamics remain poorly understood in the remote marine boundary layer (MBL) (Galbally et al. 2000; Read et al. 2008; von Glasow 2008). Compared to continental regions, the chemistry governing O_3 formation and destruction is different over the oceans. Therefore, in the MBL mechanisms of O_3 production and destruction must be understood and quantified so that the tropospheric O_3 budget can be constrained (Galbally et al. 2000; Horowitz et al. 2003; Yang et al. 2005; von Glasow 2008). Due to logistical challenges, atmospheric measurements of reactive trace gases are rarely reported for the remote MBL. To improve estimates of the global O_3 budget, long-term studies over the open ocean are essential (Lelieveld et al. 2004; von Glasow 2008).

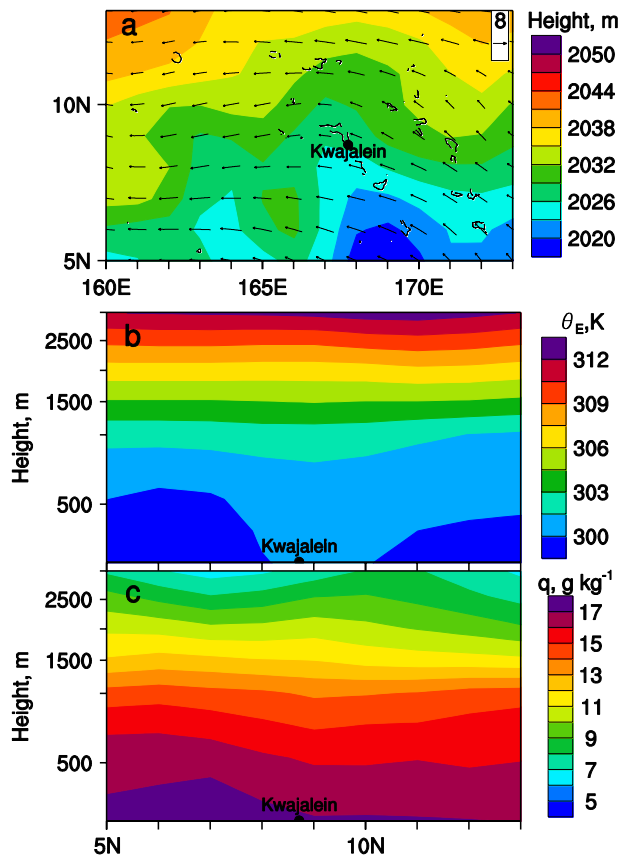
Because of low concentrations of nitrogen oxides, photochemical destruction and reactions with halogens (especially bromine) represent the major O_3 sinks in the MBL (Johnson et al. 1990; Lee et al. 2009). Deep moist convection, associated with upward and downward transport of air masses, can also influence the spatio-temporal distribution of O_3 in the lower tropical atmosphere (Betts et al. 2002; Grant et al. 2008; Sahu and Lal 2006; Hu et al. 2010b). Over the open oceans, previous studies (Solomon et al. 2005; Kley et al. 1996; Takashima et al. 2008) indicated that due to upward transport of low- O_3 air masses associated with convection, upper air layers can be at times devoid of O_3 . To date, little information exists on the O_3 transport associated with downdrafts of mesoscale convective systems in the oceanic marine boundary layer. Thus, the present study investigates the meteorological conditions governing the diurnal patterns of O_3 in the open central Pacific Ocean. An additional goal of this study is to estimate the downward O_3 transport associated with moist convection and define the O_3 changes in the MBL as a function of the propagation velocity of convective storms. The results reported herein provide insights to advance the current understanding of O_3 sinks and sources in the marine atmosphere.

2 Research methods

2.1 In-situ measurements

The field study took place during July to September 1999 at Kwajalein Atoll in the Republic of the Marshall Islands (Fig. 1a) and was part of the NASA-funded KWAJEX (Kwajalein Experiment) ground validation campaign (Yüter et al. 2005). The KWAJEX campaign was designed to validate radar observations made by the Tropical Rainfall Measurement Mission (TRMM) satellite. A 12-m flux tower, located 3 m from the high tide line of Meck Island (latitude $8^\circ 43' N$, longitude $167^\circ 44' E$), served as a platform to deploy sensors and thus define the state of the lower atmosphere. Air temperature (at 1.5, 3.0, 5.0, 7.0, and 8.5 m above ground), water vapor mixing ratio (at 5.0, and 9.0 m above ground), wind speed (WSP) and direction (at 10.0 m above the ground), and atmosphere pressure (at 1.5 m above ground) were acquired every 2 s. Sensors were connected to and resulting

Fig. 1 **a** Map of geopotential heights and wind vectors at 800 hPa over Kwajalein, **b** equivalent potential temperature (θ_E), and **c** specific humidity for the south-north cross section through Kwajalein on August 14, 1999 obtained from the National Centers for Environmental Prediction (NCEP) global forecast system (GFS) final (FNL) operational global analysis data. Reference wind vector of 8 ms^{-1} is provided in the up-right corner of Fig. 1a



information was stored on a data logger (model CR7, Campbell Scientific Inc., Logan, UT). Components of the surface energy balance were measured, including the incoming and outgoing solar and thermal energy fluxes (model CNR1, Kipp and Zonen, Delft, Netherlands). An eddy covariance system comprised of a sonic anemometer (model WindMaster Pro, Gill Instruments Ltd., Hampshire, England) and a water vapor/carbon dioxide infrared gas analyzer (model LI-6262, LiCor Inc., Lincoln, NB) made fast-response measurements at 9.5 m above the ground. A tethered sonde system consisting of balloon, hydraulic winch, instrumented sonde, and on-board data acquisition system was deployed. One complete ascending and descending profile was made every 3 h at 03:00, 06:00, 09:00, 12:00, 15:00, 18:00, 21:00, and 2400 UTC (Universal Time Coordinate), weather permitting. Data were logged onboard and transferred to a computer after each sounding. With a constant rate of rise and descent of 1 ms^{-1} , a 30-m^3 tethered balloon was used to lift a single sonde to a maximum altitude of 1,500 m. The sonde was equipped with sensors to measure horizontal wind speed and direction, atmospheric pressure, air temperature, and relative humidity every 2 s, corresponding to 2-m vertical resolution. Such information was necessary to estimate the vertical profiles of variables such as specific humidity, wind speed, and virtual potential temperature.

Ozone mixing ratios were measured at 2 m above the surface. Air was drawn through Teflon tubing and into a TECO gas analyzer (model TECO 49 C, Thermal Environmental Instruments, Franklin, MA). The air-sampling inlet had a filter holder with a filter

membrane (1 μm in pore size) to keep the tubing free of dust and sea salt particles. The O_3 gas analyzer (the instrument has a quoted response time of 20 s) made measurements every second and 1-minute O_3 averages were generated and stored on a logger (model 21X, Campbell Scientific, Logan, UT). Before and after the field campaign, the O_3 gas analyzer was calibrated. Instrument span was verified once a week.

2.2 Zero-dimensional simulations

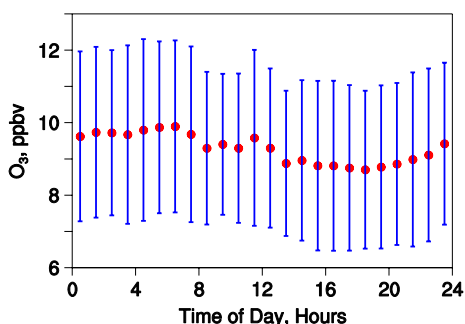
To investigate the destruction of O_3 due to gas phase reactions, simulations were conducted using a zero-dimensional version of the model of Regional Atmospheric Chemistry Mechanism (RACM) photochemical mechanism (Stockwell et al. 1997). The RACM mechanism was intended to be valid for remote to polluted conditions; however, the original mechanism did not include the bromide chemistry. To estimate the contribution of bromide chemistry to the destruction of O_3 during daytime in the MBL, the RACM model was extended to include the bromide chemistry. Simulations were also conducted using the extended RACM model to quantify the impact of bromide chemistry.

3 Results

During summer of 1999, the Kwajalein Island was located at or near the northern edge of the western Pacific Ocean inter-tropical convergence zone (ITCZ), which was centered between 5° and 10° N (Sobel et al. 2004; Yuter et al. 2005). In the Kwajalein region, weather conditions were dominated by westward-propagating synoptic scale disturbances, punctuated by mesoscale convective storms (Sobel et al. 2004). For example, on August 14, 1999 the geopotential height map at 800 hPa (Fig. 1a) showed a westward-propagating synoptic system near Kwajalein. In the absence of regional convection, equivalent potential temperature (Θ_E) increased with height (Fig. 1b), implying that the lower atmosphere over the ocean was mostly stable. Water vapor was mostly confined in the lower atmosphere (Fig. 1c). At higher altitude (>3 km), specific humidity was less than 6 g kg^{-1} .

In the absence of moist convection, during the period of observations daily O_3 mixing ratios exhibited diurnal variations amounting to 1–3 ppbv (around the mean). Ozone mixing ratios decreased after sunrise, reached minimum in the afternoon, and increased during nighttime (Fig. 2). Mean O_3 mixing ratio during nighttime and morning was approximately 10 ppbv. During the afternoon hours, the O_3 mixing ratio decreased and reached minimum values of 9 ppbv by 16:00 and 19:00 h (local time, LT) likely in response to photochemical sinks. Based on sonde and aircraft measurements in remote oceanic environments, other

Fig. 2 Mean diurnal variation of O_3 mixing ratio and standard deviation at Kwajalein during July, August and September 1999



studies (Kley et al. 1996; Singh et al. 1996; Takashima et al. 2008) also reported similar O_3 patterns in the lower atmosphere. The observed diurnal O_3 patterns reflect the reduced contribution of precursors such as nitrogen oxides and volatile organic compounds.

During calm days without disturbance of convective weather systems, the O_3 mixing ratios in the afternoon were lower by about 3 ppbv than those levels observed during nighttime or early morning. Figure 3 shows two examples for July 28 and August 15, 1999. Throughout the course of these days, the zonal wind speed exhibited little variability and stayed around $3\text{--}5\text{ ms}^{-1}$. Previous studies (e.g., Oltmans 1981; Johnson et al. 1990; Thompson et al. 1993; Rhoads et al. 1997; Lal et al. 1998; Dickerson et al. 1999; Nagao et al. 1999b; Bhugwant and Bremaud 2001; Bhugwant et al. 2001; Watanabe et al. 2005) also documented similar diurnal variations of O_3 mixing ratio in the MBL. As shown below, chemical reactions and turbulent transport explained the diurnal patterns of O_3 levels.

Diurnal variations of surface O_3 mixing ratios over the Pacific Ocean are different from those ordinarily observed in the CBL where sufficient precursors prevail to form O_3 via photochemical processes. The O_3 minimum in the afternoon over the ocean can be related to chemical sinks that are different from those associated with continental photochemical

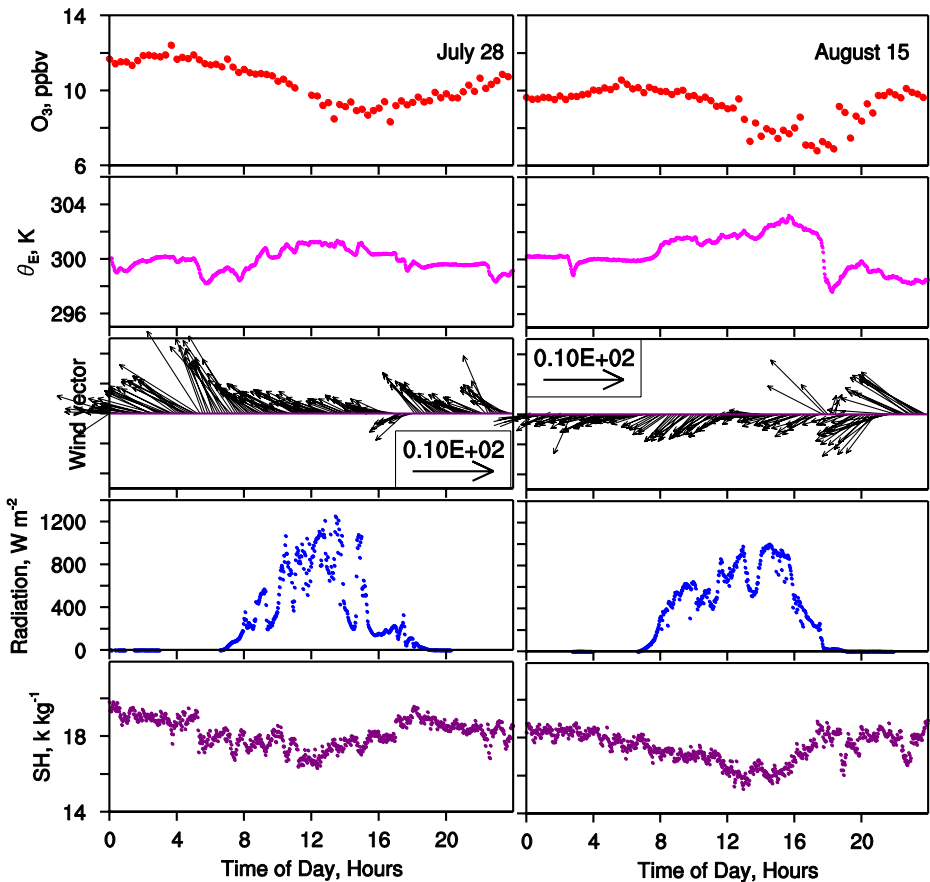
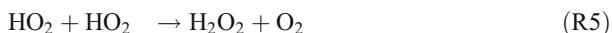
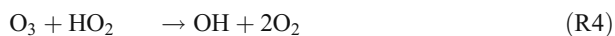
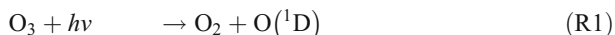


Fig. 3 Ozone mixing ratio, equivalent potential temperature (Θ_E), wind vector, incoming solar radiation, and specific humidity (SH) at Kwajalein on (left to right) July 28 and August 15, 1999

processes (Johnson et al. 1990; Ayers et al. 1992; Dickerson et al. 1999). The conventional chemistry for tropospheric O₃ destruction can be summarized via reactions R1 to R5:



Over the ocean, the mixing ratio of nitrogen oxides is low (Torres and Thompson 1993). Under such conditions, the OH radical cannot recycle O₃ and thus photochemical reactions destroy O₃ in the MBL (Liu et al. 1983; Thompson and Lenschow 1984; Thompson et al. 1993; Singh et al. 1996; Stickler et al. 2007). A zero-dimensional model, based on the RACM photochemical mechanism (Stockwell et al. 1997), was applied to estimate O₃ depletion rate due to photolysis of O₃ and reactions with OH and HO₂. The zero-dimensional RACM model was applied to a clear day in Kwajalein. The initial mixing ratio values for O₃, NO, NO₂ were set as 10 ppbv, 5 pptv, 10 pptv. The model was integrated from 5:00 LT to 19:00 LT. In addition to a control simulation, two other sensitivity simulations were conducted to estimate the contribution to the destruction of O₃ from the photolysis reaction and reactions with OH and HO₂. The configuration of the simulations is summarized in Table 1. These simulations implied photolysis of O₃ (O₃ + hν = O(¹D) + O₂) and its reactions with OH and HO₂ decreased O₃ mixing ratios by 0.9 ppbv (i.e., 10.4–9.4 ppbv) during the daytime. The reactions with OH and HO₂ accounted for 0.3 ppbv (i.e., 9.7–9.4 ppbv).

Hydrogen oxides (HO_x = OH + HO₂) alone could not account for the observed amplitude of O₃ diurnal variation over the ocean (de Laat et al. 1999; Dickerson et al. 1999; Nagao et al. 1999a; Galbally et al. 2000; von Glasow et al. 2002). Sea-salt particles can release reactive bromine (Br) through heterogeneous reactions (Sander et al. 2003; Hunt et al. 2004; Simpson et al. 2007) and then lead to surface O₃ destruction during daytime (Fan and Jacob 1992; Vøgt et al. 1996; Jacob 2000; Hara et al. 2010). Bromine can provide an additional photochemical O₃ sink through reactions R6 to R9 (Dickerson et al. 1999;

Table 1 Configurations for the simulations with the zero-dimensional model

Simulations	Configuration	O ₃ mixing ratios at 19:00 LT, ppbv
Control simulation	Default reactions included in RACM	9.4
Sensitivity simulation 1	Turn off O ₃ + hν → O(¹ D) + O ₂	10.4
Sensitivity simulation 2	Turn off O ₃ + HO → HO ₂ + O ₂ and O ₃ + HO ₂ → HO + 2.OO ₂	9.7

Jacob 2000; Foster et al. 2001; Hara et al. 2010):



Previous studies (von Glasow et al. 2002; Read et al. 2008) indicated that bromine reactions accounted for 30–47% of the total chemical O_3 destruction in the MBL. Thus, the O_3 minimum in the afternoon is likely due to the chemical reactions involving both HO_x and bromine. Nagao et al. (1999a) studied a three-year O_3 record obtained at an island in the sub-tropical northwestern Pacific Ocean and found that HO_x and bromine played different roles in destroying O_3 during different times of day. The HO_x - O_3 destruction mechanism mainly results from ultraviolet photolysis of O_3 and subsequent catalytic reaction with HO_x (R2 and R3). Therefore, the HO_x - O_3 destruction mechanism plays a dominant role around midday while reactive bromine-containing gases accumulate in the MBL during nighttime (Hunt et al. 2004). Shortly after sunrise, bromine compounds can be rapidly photolyzed to produce bromine atoms (von Glasow 2008). Bromine chemistry plays a dominant role in destroying O_3 in the morning (Nagao et al. 1999a; Galbally et al. 2000; Saiz-Lopez et al. 2004). In order to demonstrate the O_3 temporal tendency, mean diurnal variations of the time derivative of O_3 mixing ratio ($\delta[\text{O}_3]/\delta t$) are plotted in Fig. 4, in which negative values of $\delta[\text{O}_3]/\delta t$ indicate O_3 destruction. During 06:00 to 18:00 LT O_3 was destroyed, except 10:00 LT. Nagao et al. (1999a) reported a similar pattern of $\delta[\text{O}_3]/\delta t$ for the sub-tropical northwestern Pacific Ocean during August. In the present study, the O_3 destruction during the early morning and the rest of the daytime can be ascribed to bromine and HO_x reactions.

To investigate the role of bromide chemistry in the daytime O_3 depletion in Kwajalein, an extended zero-dimensional RACM model was developed to include the bromide chemistry (see Table 2). As summarized in Table 1, the extended RACM model was integrated from 5:00 LT to 19:00 LT. The initial Br_2 mixing ratio was set as 10 pptv based on results reported by Hunt et al. (2004). Shortly after the sunrise around 6:00 LT, photolysis (R6) converted all Br_2 to bromide atom and O_3 was depleted through R7.

Fig. 4 Average diurnal variation of ozone change rate ($\delta[\text{O}_3]/\delta t$) and standard deviation at Kwajalein during the summer of 1999

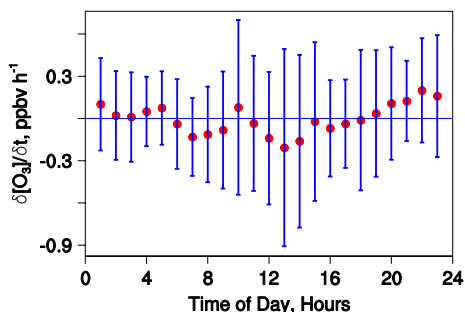


Table 2 Kinetic data related to bromine used in the extended zero-dimensional model

Photolysis reaction	Photolysis frequency, s^{-1}	Reference
$\text{HOBr} + h\nu = \text{Br} + \text{HO}$	7.9×10^{-4}	Michalowski et al. (2000)
$\text{Br}_2 + h\nu \rightarrow 2 \text{Br}$	3.02×10^{-2}	Jacobson (2005)
$\text{BrO} + h\nu \rightarrow \text{Br} + \text{O}^3\text{P}$	3.82×10^{-3}	Jacobson (2005)
Bimolecular reaction	Reaction rate constant, $\text{cm molecule}^{-1} \text{s}^{-1}$	
$\text{Br} + \text{O}_3 \rightarrow \text{BrO} + \text{O}_2$	$1.7 \times 10^{-11} e^{(-800/T)}$	Jacobson (2005)
$\text{BrO} + \text{O}_3 \rightarrow \text{Br} + \text{O}_2$	$1.0 \times 10^{-12} e^{(-3200/T)}$	Jacobson (2005)
$\text{BrO} + \text{HO}_2 \rightarrow \text{HOBr} + \text{O}_2$	$3.4 \times 10^{-12} e^{(540/T)}$	Jacobson (2005)
$\text{Br} + \text{HO}_2 \rightarrow \text{HBr} + \text{O}_2$	$1.5 \times 10^{-11} e^{(-600/T)}$	Jacobson (2005)
$\text{HBr} + \text{HO} \rightarrow \text{Br} + \text{H}_2\text{O}$	1.1×10^{-11}	Read et al. (2008)
$\text{BrO} + \text{NO} \rightarrow \text{Br} + \text{NO}_2$	$8.8 \times 10^{-12} e^{(260/T)}$	Read et al. (2008)
$\text{BrO} + \text{BrO} \rightarrow 2 \text{Br} + \text{O}_2$	$2.4 \times 10^{-12} e^{(40/T)}$	Jacobson (2005)
$\text{BrO} + \text{BrO} \rightarrow \text{Br}_2 + \text{O}_2$	$2.8 \times 10^{-14} e^{(860/T)}$	Jacobson (2005)
$\text{Br} + \text{HCHO} \rightarrow \text{HBr} + \text{CO} + \text{HO}_2$	$1.7 \times 10^{-11} e^{(-800/T)}$	Jacobson (2005)

Because R6 and R7 occurred so quickly after sunrise, BrO showed a peak right after sunrise (Fig. 5). Ozone was 24 depleted to 8.9 ppbv at 19:00 LT. The zero-dimensional model results were consistent with those 25 reported in Saiz-Lopez et al. (2006) in terms of the diurnal pattern of O₃, BrO and Br₂. Compared with the control simulation (Table 1), the exclusion of bromide chemistry caused an underestimation of O₃ loss by 0.5 ppbv (45%). Such estimation was close to that estimated in Read et al. (2008). The simulated O₃ destruction rate during the daytime with and without bromide chemistry is compared in Fig. 6. When the bromide chemistry was excluded, the change of O₃ destruction rate followed the change of photolysis rate (also change of OH mixing ratio) and reached peak value during the middle of the day. When the bromide chemistry was included, the O₃ destruction rate almost doubled during the daytime and it showed a spike in the early morning. The simulated spike of O₃ destruction rate in the early morning is consistent with the observations shown in Fig. 4. The time of the spike of O₃ destruction rate matches that of the spike of the BrO values shown in Fig. 5. Thus, the zero-dimensional model simulation confirmed that the spike of O₃ destruction in the early morning occurred because the accumulated Br₂ during nighttime in the MBL was photolyzed rapidly after sunrise and the following bromide catalytic reactions destroyed O₃.

Fig. 5 Simulated time series of ozone (O₃), bromine atoms (Br), hydroxyl radical (OH), and bromine monoxide (BrO) mixing ratios during the daytime using the extended zero-dimensional model

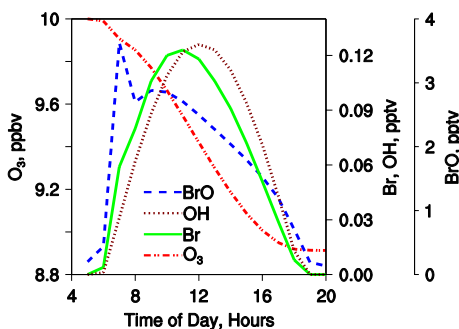
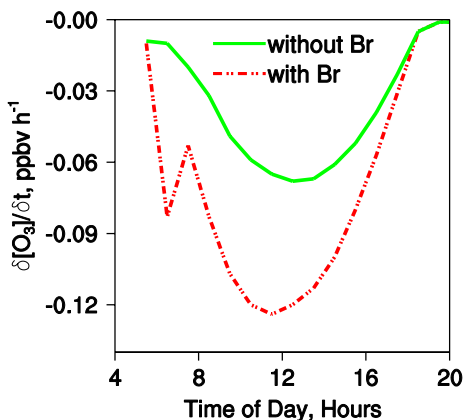


Fig. 6 Simulated destruction rate of ozone (O_3) during the daytime in the MBL using the zero-dimensional model (without bromide chemistry) and the extended zero-dimensional model (with bromide chemistry)



Chemical reactions alone cannot explain the observed O_3 temporal patterns. Ozone mixing ratios increased during the nighttime in response to the lack of photolytic reactions (Figs. 2 and 3). Transport of O_3 -richer air from the free troposphere to the surface likely explained the O_3 increases observed during the nighttime (Ayers et al. 1997; Bremaud et al. 1998; Monks et al. 2000; Chand et al. 2003; Sigler et al. 2002). Skewness of specific humidity, q , $\left(S_q = \overline{q'^3} / (\overline{q'^2})^{3/2}\right)$, q' represents the specific humidity perturbation from the mean) can be used as a proxy to investigate the O_3 vertical transport process (Deardorff 1974; Lambert et al. 1999). Tethered balloon measurements of q profiles and associated S_q values were estimated for the month of August 1999 to determine the influence of vertical transport on the O_3 temporal variability (in the absence of storms, the height of the mixed layer (z_i) ranged from 400 to 450 m and average q values in the mixed layer reach 20 g kg^{-1} , Fig. 7). Positive S_q values were estimated for the lower part of the MBL (below 280 m) whereas negative S_q values were observed in the upper part of the MBL. Negative S_q values in the upper part of the MBL indicated that the dry air entrained from the free troposphere became stretched into narrow downward streamers. This finding indicated that vertical transport contributed to the replenishment of O_3 in the upper MBL as reported in previous studies (Lambert et al. 1999). The low S_q values below 280 m indicated that more symmetric turbulence was likely responsible for vertical mixing in the lower part of the MBL.

Entrainment of free tropospheric air into the mixed layer and surface deposition can contribute to O_3 temporal patterns. Under steady state and homogeneous (non-advective) conditions, the amount of O_3 entrained into the MBL can be estimated from (1)

$$[O_3]_{Ent} = \frac{w_e([O_3]_{FT} - [O_3]_{BL})}{z_i} \quad (1)$$

where $[O_3]_{Ent}$ is the average change rate of the O_3 mixing ratio in the MBL due to the entrainment, w_e is the entrainment velocity, $[O_3]_{FT}$ is the O_3 mixing ratio in the free troposphere, $[O_3]_{BL}$ is the O_3 mixing ratio in the MBL and z_i is the mixed layer height (Monks et al. 2000). Since no O_3 profile data were available for MBL over Kawajlein, the $[O_3]_{BL}$ and $[O_3]_{FT}$ values needed to apply Eq. (1) were obtained from ozonesondes obtained in the American Samoa (14.23° S , 170.56° W) during April and May of 1999. The $[O_3]_{FT}$ was normally larger than $[O_3]_{BL}$ (Thompson et al. 2003). The average $[O_3]_{FT}[O_3]_{BL}$ over the equatorial Pacific Ocean in summer was about 2 ppbv. The value of w_e over the ocean was

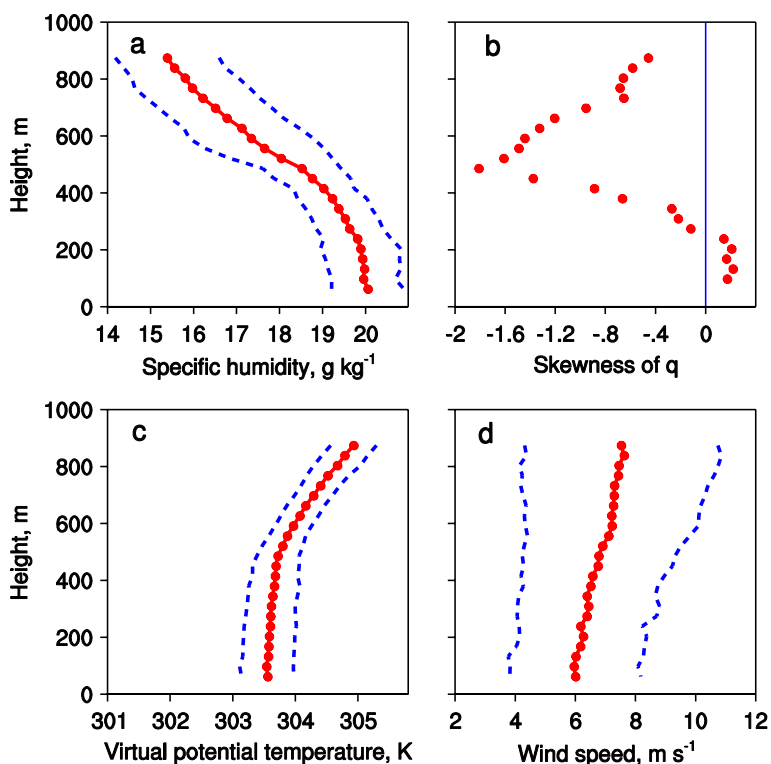
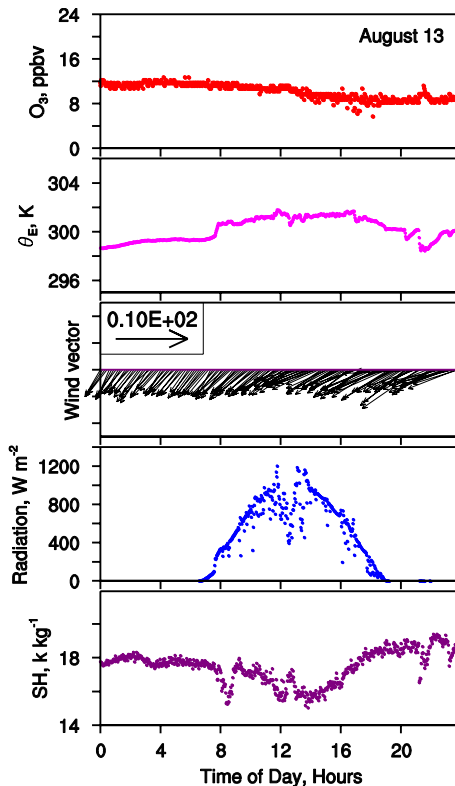


Fig. 7 Profiles of (a) mean specific humidity during August 1999 in Kwajalein, (b) skewness of specific humidity, (c) mean virtual potential temperature, and (d) mean wind speed. One standard deviations of specific humidity, virtual potential temperature and wind speed are shown with the dashed lines in (a), (c) and (d)

reported to be 4–14 mm s^{-1} (Boers et al. 1998; Bremaud and Taupin 1998; Bremaud et al. 1998; Stevens et al. 2003). Using the tethered balloon data (Fig. 7), the average z_i ranged from 500 to 800 m. Therefore, the estimated $[\text{O}_3]_{\text{Ent}}$ varied from 0.04 to 0.2 ppb hr^{-1} . With this increasing rate, due to the entrainment process, the nighttime surface O_3 mixing ratio increased after sunset to the O_3 levels observed at sunrise (Figs. 2 and 3). Thus, the photochemical reactions and the recovery mechanism during nighttime contributed to the diurnal variation of surface O_3 mixing ratio shown in Fig. 2. In addition to the enhanced O_3 destructive reactions in the afternoon, dry deposition was another process contributing to reductions in surface O_3 mixing ratios (Singh et al. 1996; Fairall et al. 2007). Dry deposition was estimated to account for 13% of total O_3 loss in summer in the remote MBL when bromine chemistry was neglected (Monks et al. 2000; Ganzeveld et al. 2009).

Thermodynamic conditions of the MBL exerted control on the O_3 temporal variability. For example, Figs. 8 and 9 illustrate examples of O_3 levels on August 13 and 19, 1999 (and associated meteorological conditions: equivalent potential temperature, wind vector, solar irradiance, and specific humidity) exhibiting little diurnal variation. During the daytime, O_3 mixing ratios slowly decreased with time. However, after sunset O_3 levels did not increase to reach the mixing ratios observed around sunrise. This may be because the downward O_3 transport due to entrainment was not as strong as that on days such as July 28 and August 15, 1999. The thermodynamic attributes of the MBL on August 13, 15 and 19, 1999 were

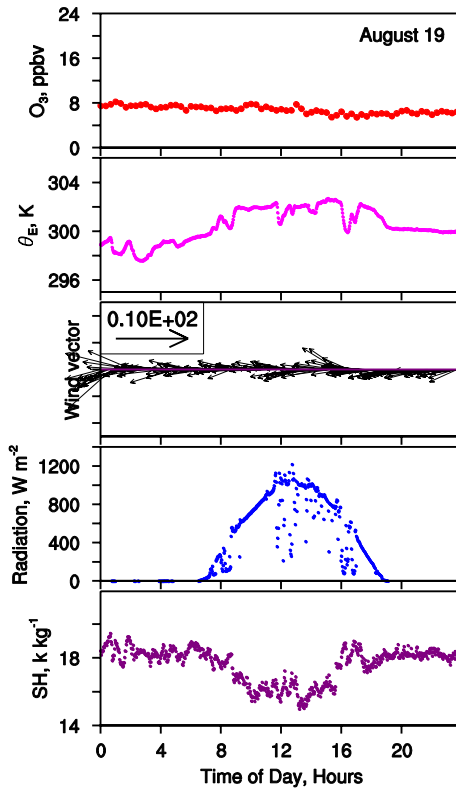
Fig. 8 Ozone mixing ratio, equivalent potential temperature (Θ_E), wind vector, incoming solar radiation, and specific humidity (SH) at Kwajalein for the case of ozone decreasing with time (during August 13, 1999)



investigated from the tethersonde data (data were not available on July 28, 1999) (Fig. 10). The 1.5-theta-increase method (Nielsen-Gammon et al. 2008; Hu et al. 2010a) was used to diagnose mixed layer height from the potential temperature profile. The 1.5-theta-increase method defined the mixed layer height as the level at which the potential temperature first exceeded the minimum potential temperature within the boundary layer by 1.5 K. Inferred from the tethersonde data, the mixed layer height was greater at 22:00 LT on August 13 (713 m) and August 19 (773 m) than that on August 15 (698 m). In addition, specific humidity and wind speed across the MBL top exhibited little gradients on August 13 and August 19, 1999 (Fig. 10). These MBL dynamic conditions (Fig. 10) likely became ineffective in downwardly transporting O_3 rich air to the surface. Also, for both days (Figs. 8 and 9) the friction velocity (u_*) was low ($<0.2 \text{ ms}^{-1}$) in response to weaker mechanical turbulence. Weaker turbulence and reduced vertical mixing combined with higher MBL height implied less increase of surface O_3 due to entrainment.

Mesoscale convective storms modulated the diurnal O_3 patterns. For example, between 21:00 and 22:00 LT on August 13, 1999, O_3 mixing ratios suddenly increased (2–3 ppbv) in response of a storm that caused rapid decreases in Θ_E and increases in wind speed (Fig. 8). Two additional cases (Figs. 11 and 12) showed greater increases of O_3 (amounting to 6–12 ppb on July 25 and August 10, 1999). On July 25, 1999 the O_3 increase occurred during the nighttime (around 19:00 LT) while that on August 10 happened during the daytime (around 11:00 LT). The O_3 increases near the surface occurred in response to the downward transport associated with convection that brought air from the upper air layers down to the surface with lower Θ_E and specific humidity. The surface Θ_E decreased in response to the evaporative

Fig. 9 Ozone mixing ratio, equivalent potential temperature (Θ_E), wind vector, incoming solar radiation, and specific humidity (SH) at Kwajalein for the case of ozone decreasing with time (during August 19, 1999)



cooling associated with rainfall. At times the reduction in surface Θ_E exceeded 4 K which agreed with previously reported findings in tropical maritime environments (Schumacher et al. 2007). For the case of July 25, 1999 there was a rapid increase of wind speed during convection while the change of wind speed for the case of August 10, 1999 was not substantial. Rainfall was associated with the case of July 25, 1999 while no rainfall occurred during the convective case of August 10, 1999 (data not shown). Previous studies (Betts et al.

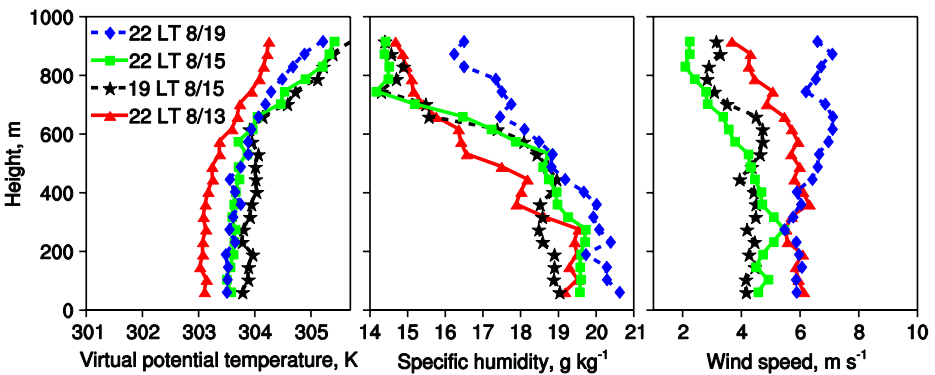
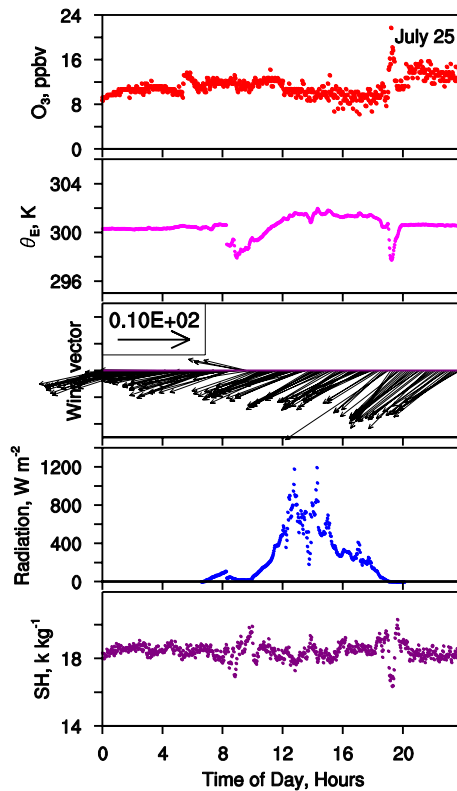


Fig. 10 Profiles of (*left*) virtual potential temperature, (*middle*) specific humidity, and (*right*) wind speed (WSP) during nighttime on August 13, 15, and 19, 1999 in Kwajalein

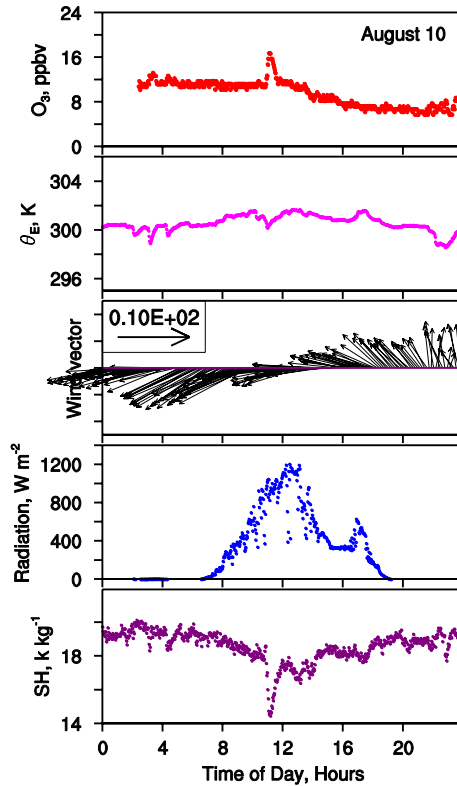
Fig. 11 Ozone mixing ratio, equivalent potential temperature (Θ_E), wind vector, incoming solar radiation, and specific humidity (SH) at Kwajalein for storm case on July 25, 1999



2002; Grant et al. 2008; Hu et al. 2010b) reported that downdrafts associated with moist convection over continental regions increased the ground-level O_3 by 10–30 ppb and lasted for a few hours (>2 h). In contrast, over the ocean the elevated O_3 levels after convection decreased to the level before convection in a short time period (less than 1 h) (Figs. 11 and 12). These differences likely resulted due to the different O_3 distribution patterns in the free troposphere (Thompson and Lenschow 1984), different strength of convective storms (Zipser and Lutz 1994), and different air chemistry (Ayers et al. 1992). Over the equatorial Pacific Ocean marine boundary layer, the O_3 mixing ratio in the free troposphere is relatively low (e.g., <20 ppbv, Kley et al. 1996). Thus, the free tropospheric air masses over the ocean brought down to the surface by convection contained low- O_3 air. Convective systems over tropical oceans have weaker vertical velocities than those observed over continents (Del Genio et al. 2007; Zipser and Lutz 1994). A summary of the influences of convection and storm propagating velocities on the transport of O_3 and changes in Θ_E is provided in Table 3.

During the field campaign, as documented by Sobel et al. (2004) and Yuter et al. (2005), one of the largest rainfall events occurred on August 12, 1999. Radar reflectivity values showed that the study region became cloudy during most of August 12, 1999. The incoming solar radiation reaching the surface was less than 100 W m^{-2} (Fig. 13). Under such conditions, the photolytic reactions and subsequent HO_x and bromine reactions were suppressed. This was the likely reason why the O_3 decreases during the daytime (Figs. 2 and 3) did not occur on August 12, 1999. During August 12, 1999 the mixed layer height decreased in response to the disturbance caused by the storm. Diagnosed from the profiles

Fig. 12 Ozone mixing ratio, equivalent potential temperature (Θ_E), wind vector, incoming solar radiation, and specific humidity (SH) at Kwajalein for storm case on August 10, 1999

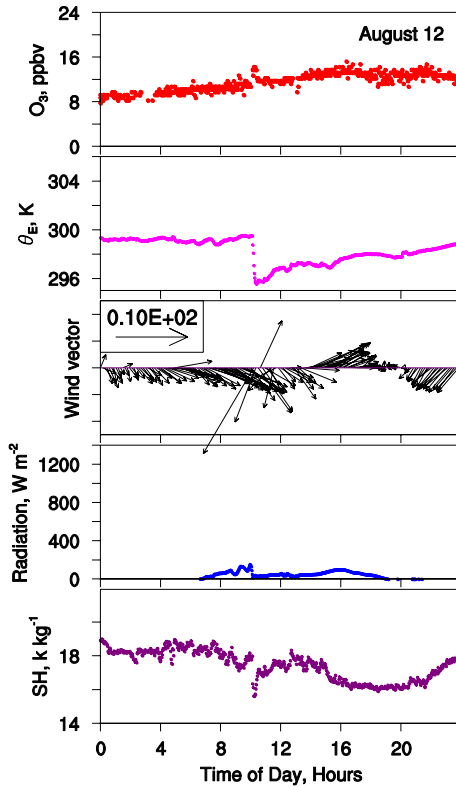


of virtual potential temperature (Fig. 14), the mixed layer height changed from about 800 m at 01:00 LT on August 12 to about 300 m at 04:00 LT on August 13, 1999. The presence of clouds enhanced turbulence in the MBL relative to clear conditions (Betts and Boers 1990), which entrained more O_3 -richer air into the MBL and augmented the air mass transport to the lower MBL. Elevated friction velocity ($>0.4 \text{ ms}^{-1}$) on August 12, 1999 (data not shown) implied greater turbulent transport. Surface specific humidity decreased between 15:00 LT and 21:00 LT (Fig. 13) in response to the downward transport of free tropospheric air, which contained less water vapor. Enhanced turbulence and reduced depth of the MBL likely enhanced downward O_3 transport to the surface from the free troposphere; thus, the surface O_3 mixing ratio increased during the daytime of August 12, 1999.

Table 3 Maximum wind speed (WSP), magnitude of O_3 change ($\Delta[O_3]$), magnitude of Θ_E change ($\Delta[\Theta_E]$), duration (τ) of O_3 enhancement, and occurrence of precipitation associated with four representative convective storms observed in Kwajalein on July 25, August 10, 12, 13, 1999

Cases	Maximum WSP, m s^{-1}	$\Delta[O_3]$, ppbv	$\Delta[\Theta_E]$, $^{\circ}\text{C}$	τ , minutes	Precipitation occurred?
July 25	17.3	12	3.0	45	Yes
August 10	12.2	6	1.2	45	No
August 12	15.3	3	3.9	30	Yes
August 13	13.4	3	1.6	50	Yes

Fig. 13 Ozone mixing ratio, equivalent potential temperature (θ_E), wind vector, incoming solar radiation, and specific humidity (SH) at Kwajalein for the case with increasing O_3 on August 12, 1999



The relationship between mixed layer height and surface O_3 mixing ratio was further investigated. The mixed layer varied between 250 and 850 m. Estimated mixed layer heights and measured O_3 mixing ratios exhibited a linear relationship (Fig. 15), with a correlation coefficient of -0.43 . The relatively low correlation coefficient (-0.43) implied

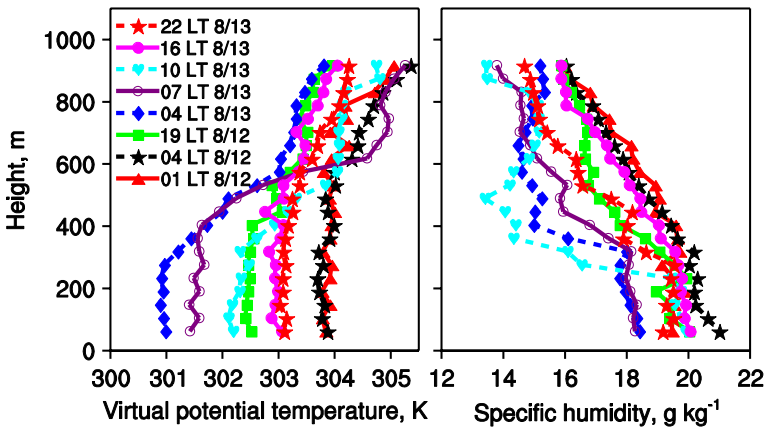
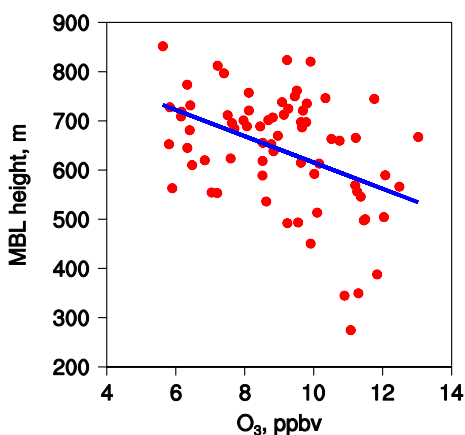


Fig. 14 Profiles of (*left*) virtual potential temperature and (*right*) specific humidity on August 12 and 13, 1999 in Kwajalein

Fig. 15 Correlation between observed MBL height and O_3 during the summer of 1999. The correlation coefficient is -0.43 . The blue line represents the linear regression of all data points



that the boundary layer height was only one of the factors that affected surface O_3 mixing ratios. Higher O_3 mixing ratios were associated with shallower mixed layers. Conversely, lower O_3 mixing ratios occurred when the mixed layer became deep.

4 Summary and conclusions

Over the equatorial Pacific Ocean O_3 mixing ratios exhibited minimal diurnal variation, with an average of $9\text{--}10 \pm 2.5$ ppbv. Following sunrise, O_3 mixing ratios decreased, reached minimum in the afternoon, and increased in the evening. Peak-to-peak amplitudes of O_3 diurnal variation ranged from 1 to 3 ppbv. Diurnal variations of O_3 in the marine mixed layer were ascribed to a combination of chemistry, entrainment of free-tropospheric air into the mixed layer, and downward transport associated with moist convection.

The present results provide evidence that reactions of O_3 with bromine and HO_x exerted control on the diurnal variation of O_3 in the marine boundary layer, leading to an O_3 minimum in the afternoon. Under undisturbed conditions (i.e., no rain events), the mixed layer reached heights ranging from 500 to 800 m and remained largely invariant with time. Additionally, the top of the mixed layer exhibited a well-defined temperature discontinuity, which defined the “capping” temperature inversion and separated MBL air from free tropospheric air. Due to entrainment of air from the free troposphere to the mixed layer, O_3 was transported down to the surface. This transport process increased O_3 by as much as 0.04 to 0.2 ppbv per hour, thereby influencing the observed diurnal O_3 patterns. During the nighttime, due to reduced chemical sinks, the transport of O_3 -richer air from the free troposphere to the surface became more evident and partly explained the increases in surface O_3 .

In the presence of convection, downward transport of O_3 -richer free tropospheric air increased surface O_3 mixing ratio, while surface equivalent potential temperature and specific humidity concurrently decreased in response to evaporative cooling and transport of dry air from the free troposphere. Compared to continental regions, where the increased O_3 due to convection could be maintained for several hours following the storms, over the ocean the elevated O_3 mixing ratios after convection was relatively short lived, lasting less than 1 h. The magnitude of the sudden increase of surface O_3 due to convection over the ocean was smaller (3–12 ppbv) than that observed over the continent regions (as high as 20–30 ppbv). The differences can be ascribed to the distribution of O_3 in the lower

troposphere. Over the ocean, the free troposphere has lower O₃ mixing ratios (<20 ppbv) than those observed over the continent (>40 ppbv). Moreover, convection is stronger and deeper over continent regions than over oceans.

The current findings indicate that both entrainment of relatively O₃-richer air from the free troposphere as well as storm-related convective activity play dominant roles in surface-level O₃ dynamics over tropical oceans, just as they do over continental surfaces. The observations reported in this study were conducted in the remote ocean, which is devoid of continental pollution. Results apply to the open ocean, a major sink region for tropospheric O₃. Thus, the O₃ levels and source/sink mechanisms reported in this study may be necessary to develop a more complete understanding of the global O₃ budget and therefore the role played by O₃ in atmospheric chemistry and climate.

Acknowledgements NASA provided funding for the field research related to the KWAJEX project (grants NAG5-9768). Authors are grateful to Michael Garstang, John Deary, Ryan Heitz, and Oliver W. Frauenfeld for their collaboration with the field research. Discussions with Tianle Yuan were helpful.

References

- Ayers, G.P., Penkett, S.A., Gillet, R.W., Bandy, B., Galbally, I.E., Meyer, C.P., Elsworth, C.M., Bentley, S.T., Forgan, B.W.: Evidence for photochemical control of ozone concentrations in unpolluted marine air. *Nature* **360**, 446–449 (1992)
- Ayers, G.P., Granek, H., Boers, R.: Ozone in the marine boundary layer at Cape Grim: model simulation. *J. Atmos. Chem* **27**, 179–195 (1997)
- Betts, A.K., Boers, R.: A cloudiness transition in a marine boundary layer. *J. Atmos. Sci.* **47**, 1480–1497 (1990)
- Betts, A.K., Gatti, L.V., Cordova, A.M., Silva Dias, M.A.F., Fuentes, J.D.: Transport of ozone to the surface by convective downdrafts at night. *J. Geophys. Res.* **107**(D20), 8046 (2002). doi:[10.1029/2000JD000158](https://doi.org/10.1029/2000JD000158)
- Bhugwant, C., Bremaud, P.: Simultaneous measurement of black carbon, PM₁₀, ozone and NO_x variability at a locally polluted island in the southern tropics. *J. Atmos. Chem.* **39**, 261–280 (2001)
- Bhugwant, C., Riviere, E., Keckhut, P., Leveau, J.: Variability of carbonaceous aerosols, ozone and radon at Piton Textor, a mountain site on Reunion island (South-Western Indian Ocean). *Tellus Ser. B.* **53**, 546–563 (2001)
- Boers, R., Krummel, P.B., Siems, S.T., Hess, G.D.: Thermodynamic structure and entrainment of stratocumulus over the Southern Ocean. *J. Geophys. Res.* **103**(D13), 16,637–16,650 (1998). doi:[10.1029/98JD00529](https://doi.org/10.1029/98JD00529)
- Bremaud, P.J., Taupin, F.: Cloud influence on ozone diurnal cycle in the marine boundary layer at Reunion Island. *Atmos. Res.* **48**, 285–298 (1998)
- Bremaud, P.J., Taupin, F., Thompson, A.M., Chaumerliac, N.: Ozone nighttime recovery in the marine boundary layer: measurement and simulation of the ozone diurnal cycle at Reunion Island. *J. Geophys. Res.* **103**(D3), 3463–3473 (1998). doi:[10.1029/97JD01972](https://doi.org/10.1029/97JD01972)
- Chand, D., Lal, S., Naja, M.: Variations of ozone in the marine boundary layer over the Arabian Sea and the Indian Ocean during the 1998 and 1999 INDOEX campaigns. *J. Geophys. Res.* **108**(D6), 4190 (2003). doi:[10.1029/2001JD001589](https://doi.org/10.1029/2001JD001589)
- de Laat, A.T.J., Zachariasse, M., Roelofs, G.J., van Velthoven, P., Dickerson, R.R., Rhoads, K.P., Oltmans, S. J., Lelieveld, J.: Tropospheric O₃ distribution over the Indian Ocean during spring 1995 evaluated with a chemistry-climate model. *J. Geophys. Res.* **104**(D11), 13,881–13,893 (1999). doi:[10.1029/1999JD900176](https://doi.org/10.1029/1999JD900176)
- Deardorff, J.W.: Three-dimensional numerical study of turbulence in an entraining mixed layer. *Bound. Layer Meteorol.* **7**, 199–226 (1974)
- Del Genio, A.D., Yao, M.-S., Jonas, J.: Will moist convection be stronger in a warmer climate? *Geophys. Res. Lett.* **34**, L16703 (2007). doi:[10.1029/2007GL030525](https://doi.org/10.1029/2007GL030525)

- Dickerson, R.R., Rhoads, K.P., Carsey, T.P., Oltmans, S.J., Burrows, J.P., Crutzen, P.J.: Ozone in the remote marine boundary layer: a possible role for halogens. *J. Geophys. Res.* **104**(D17), 21,385–21,395 (1999). doi:[10.1029/1999JD900023](https://doi.org/10.1029/1999JD900023)
- Fairall, C.W., Hare, J.E., Helmig, D., Ganzveld, L.: Water-side turbulence enhancement of ozone deposition to the ocean. *Atmos. Chem. Phys.* **7**, 443–451 (2007)
- Fan, S.M., Jacob, D.J.: Surface ozone depletion in Arctic spring sustained by bromine reactions on aerosols. *Nature* **359**, 524–552 (1992)
- Foster, K.L., Plastring, R.A., Bottenheim, J.W., Shepson, P.B., Finlayson-Pitts, B.J., Spicer, C.W.: The role of Br₂ and BrCl in surface ozone destruction at polar sunrise. *Science* **291**, 471–474 (2001)
- Galbally, I.E., Bentley, S.T., Meyer, C.P.: Mid-latitude marine boundary-layer ozone destruction at visible sunrise observed at Cape Grim, Tasmania, 41°S. *Geophys. Res. Lett.* **27**(23), 3841–3844 (2000). doi:[10.1029/1999GL010943](https://doi.org/10.1029/1999GL010943)
- Ganzeveld, L., Helmig, D., Fairall, C.W., Hare, J., Pozzer, A.: Atmosphere-ocean ozone exchange: a global modeling study of biogeochemical, atmospheric, and waterside turbulence dependencies. *Glob. Biogeochem. Cycles* **23**, GB4021 (2009). doi:[10.1029/2008GB003301](https://doi.org/10.1029/2008GB003301)
- Grant, D.D., Fuentes, J.D., DeLonge, M.S., Chan, S., Joseph, E., Kucera, P., Ndiaye, S.A., Gaye, A.T.: Ozone transport by mesoscale convective storms in western Senegal. *Atmos. Environ.* **42**(30), 7104–7114 (2008)
- Hara, K., Osada, K., Yabuki, M., Hashida, G., Yamanouchi, T., Hayashi, M., Shiobara, M., Nishita, C., Wada, M.: Haze episodes at Syowa station, coastal Antarctica: where did they come from? *J. Geophys. Res.* **115** (2010). doi:[10.1029/2009JD012582](https://doi.org/10.1029/2009JD012582)
- Horowitz, L.W., et al.: A global simulation of tropospheric ozone and related tracers: description and evaluation of MOZART, version 2. *J. Geophys. Res.* **108**(D24), 4784 (2003). doi:[10.1029/2002JD002853](https://doi.org/10.1029/2002JD002853)
- Hu, X.-M., Nielsen-Gammon, J.W., Zhang, F.: Evaluation of three planetary boundary layer schemes in the WRF model. *J. Appl. Meteorol. Climatol.* **49**, 1831–1844 (2010a)
- Hu, X.-M., Fuentes, J.D., Zhang, F.: Downward transport and modification of tropospheric ozone through moist convection. *J. Atmos. Chem.* **65**, 13–35 (2010b)
- Hunt, S.W., Roeselova, M., Wang, W., Wingen, L.M., Knipping, E.M., Tobias, D.J., Dabdub, D., Finlayson-Pitts, B.J.: Formation of molecular bromine from the reaction of ozone with deliquesced NaBr aerosol: evidence for interface chemistry. *J. Phys. Chem. A.* **108**, 11559–11572 (2004)
- Jacob, D.J.: Heterogeneous chemistry and tropospheric ozone. *Atmos. Environ.* **34**, 2131–2159 (2000)
- Jacobson, M.Z.: Fundamentals of atmospheric modeling second edition. Cambridge Univ. Press, Cambridge (2005)
- Johnson, J.E., Gammon, R.H., Larsen, J., Bates, T.S., Oltmans, S.J., Farmer, J.C.: Ozone in the marine boundary layer over the Pacific and Indian Oceans: latitudinal gradients and diurnal cycles. *J. Geophys. Res.* **95**(D8), 11,847–11,856 (1990)
- Kley, D., Crutzen, P.J., Smit, H.G.J., Vömel, H., Oltmans, S.J., Grassl, H., Ramanathan, V.: Observations of near-zero ozone levels over the convective Pacific: effects on air chemistry. *Science* **274**, 230–233 (1996)
- Lal, S., Naja, M., Jayaraman, A.: Ozone in the marine boundary layer over the tropical Indian Ocean. *J. Geophys. Res.* **103**(D15), 18,907–18,917 (1998). doi:[10.1029/98JD01566](https://doi.org/10.1029/98JD01566)
- Lambert, D., Durand, P., Thoumieux, F., Bénech, B., Druilhet, A.: The marine atmospheric boundary layer during SEMAPHORE: II. Turbulence profiles in the mixed layer. *Q. J. R. Meteorol. Soc.* **125**, 513–528 (1999)
- Lee, J.D., Moller, S.J., Read, K.A., Lewis, A.C., Mendes, L., Carpenter, L.J.: Year-round measurements of nitrogen oxides and ozone in the tropical North Atlantic marine boundary layer. *J. Geophys. Res.* **114**, D21302 (2009). doi:[10.1029/2009JD011878](https://doi.org/10.1029/2009JD011878)
- Lelieveld, J., Van Aardenne, J., Fischer, H., de Reus, M., Williams, J., Winkler, P.: Increasing ozone over the Atlantic Ocean. *Science* **304**(5676), 1483–1487 (2004). doi:[10.1126/science.1096777](https://doi.org/10.1126/science.1096777)
- Liu, S.C., McFarland, M., Kley, D., Zafiriou, O., Huebert, B.: Tropospheric NO_x and O₃ budgets in the equatorial Pacific. *J. Geophys. Res.* **88**(C2), 1360–1368 (1983)
- Michalowski, B.A., Francisco, J.S., Li, S.-M., Barrie, L.A., Bottenheim, J.W., Shepson, P.B.: A computer model study of multiphase chemistry in the Arctic boundary layer during polar sunrise. *J. Geophys. Res.* **105**, 15,131–15,145 (2000)
- Monks, P.S., Salisbury, G., Holland, G., Penkett, S.A., Ayers, G.P.: A seasonal comparison of ozone photochemistry in the remote marine boundary layer. *Atmos. Environ.* **34**, 2547–2561 (2000)
- Nagao, I., Matsumoto, K., Tanaka, H.: Sunrise ozone destruction found in the sub-tropical marine boundary layer. *Geophys. Res. Lett.* **26**(22), 3377–3380 (1999a). doi:[10.1029/1999GL010836](https://doi.org/10.1029/1999GL010836)

- Nagao, I., Matsumoto, K., Tanaka, H.: Characteristics of dimethylsulfide, ozone, aerosols, and cloud condensation nuclei in air masses over the northwestern Pacific Ocean. *J. Geophys. Res.* **104**(D9), 11, 675–11, 693 (1999b)
- Nielsen-Gammon, J.W., Powell, C.L., Mahoney, M.J., Angevine, W.M., Senff, C., White, A., Berkowitz, C., Doran, C., Knupp, K.: Multisensor estimation of mixing heights over a coastal city. *J. Appl. Meteorol. Climatol.* **47**, 27–43 (2008). doi:[10.1175/2007JAMC1503.1](https://doi.org/10.1175/2007JAMC1503.1)
- Oltmans, S.J.: Surface ozone measurements in clean air. *J. Geophys. Res.* **86**(C2), 1174–1180 (1981)
- Read, K.A., et al.: Extensive halogen-mediated ozone destruction over the tropical Atlantic Ocean. *Nature* **453**, 1232–1235 (2008)
- Rhoads, K.P., Kelley, P., Dickerson, R.R., Carsey, T.P., Farmer, M., Savoie, D.L., Prospero, J.M.: Composition of the troposphere over the Indian Ocean during the monsoonal transition. *J. Geophys. Res.* **102**(D15), 18,981–18,995 (1997). doi:[10.1029/97JD01078](https://doi.org/10.1029/97JD01078)
- Sahu, L.K., Lal, S.: Changes in surface ozone levels due to convective downdrafts over the Bay of Bengal. *Geophys. Res. Lett.* **33**, L10807 (2006). doi:[10.1029/2006GL025994](https://doi.org/10.1029/2006GL025994)
- Saiz-Lopez, A., Plane, J.M.C., Shillito, J.A.: Bromine oxide in the mid-latitude marine boundary layer. *Geophys. Res. Lett.* **31**, L03111 (2004). doi:[10.1029/2003GL018956](https://doi.org/10.1029/2003GL018956)
- Saiz-Lopez, A., Shillito, J.A., Coe, H., Plane, J.M.C.: Measurements and modelling of I₂, IO, OIO, BrO and NO₃ in the mid-latitude marine boundary layer. *Atmos. Chem. Phys.* **6**, 1513–1528 (2006)
- Sander, R., et al.: Inorganic bromine in the marine boundary layer: a critical review. *Atmos. Chem. Phys.* **3**, 1301–1336 (2003). doi:[10.5194/acp-3-1301-2003](https://doi.org/10.5194/acp-3-1301-2003)
- Schumacher, C., Zhang, M.H., Ciesielski, P.E.: Heating structures of the TRMM field campaigns. *J. Atmos. Sci.* **64**, 2593–2610 (2007)
- Sigler, J.M., Fuentes, J.D., Heitz, R.C., Garstang, M., Fisch, G.: Ozone dynamics and deposition processes at a deforested site in the Amazon basin. *Ambio* **31**(1), 21–27 (2002)
- Simpson, W.R., et al.: Halogens and their role in polar boundary-layer ozone depletion. *Atmos. Chem. Phys.* **7**, 4375–4418 (2007)
- Singh, H.B., et al.: Low ozone in the marine boundary layer of the tropical Pacific Ocean: photochemical loss, chlorine atoms, and entrainment. *J. Geophys. Res.* **101**(D1), 1907–1917 (1996). doi:[10.1029/95JD01028](https://doi.org/10.1029/95JD01028)
- Sobel, A.H., Yuter, S.E., Bretherton, C.S., Kiladis, G.N.: Large-scale meteorology and deep convection during TRMM KWAJEX. *Mon. Weather. Rev.* **132**, 422–444 (2004)
- Solomon, S., Thompson, D.W.J., Portmann, R.W., Oltmans, S.J., Thompson, A.M.: On the distribution and variability of ozone in the tropical upper troposphere: Implications for tropical deep convection and chemical-dynamical coupling. *Geophys. Res. Lett.* **32**, L23813 (2005). doi:[10.1029/2005GL024323](https://doi.org/10.1029/2005GL024323)
- Stevens, B., et al.: On entrainment rates in nocturnal marine stratocumulus. *Q. J. R. Meteorol. Soc.* **129**, 3469–3493 (2003)
- Stickler, A., et al.: Chemistry, transport and dry deposition of trace gases in the boundary layer over the tropical Atlantic Ocean and the Guyanas during the GABRIEL field campaign. *Atmos. Chem. Phys.* **7**, 3933–3956 (2007)
- Stockwell, W.R., Kirchner, F., Kuhn M., Seefeld, S.: A new mechanism for regional atmospheric chemistry modeling. *J. Geophys. Res.* **102**, 25,847–25,879 (1997). doi:[10.1029/97JD00849](https://doi.org/10.1029/97JD00849)
- Takashima, H., Shiotani, M., Fujiwara, M., Nishi, N., Hasebe, F.: Ozonesonde observations at Christmas Island (2°N, 157°W) in the equatorial central Pacific. *J. Geophys. Res.* **113**, D10112 (2008). doi:[10.1029/2007JD009374](https://doi.org/10.1029/2007JD009374)
- Thompson, A.M., Lenschow, D.H.: Mean profiles of trace reactive species in the unpolluted marine surface layer. *J. Geophys. Res.* **89**(D3), 4788–4796 (1984). doi:[10.1029/JD089iD03p04788](https://doi.org/10.1029/JD089iD03p04788)
- Thompson, A.M., et al.: Ozone observations and a model of marine boundary photochemistry during SAGA 3. *J. Geophys. Res.* **98**, 16,995–16,968 (1993)
- Thompson, A.M., et al.: Southern Hemisphere Additional Ozonesondes (SHADOZ) 1998–2000 tropical ozone climatology 1. Comparison with Total Ozone Mapping Spectrometer (TOMS) and ground-based measurements. *J. Geophys. Res.* **108**(D2), 8238 (2003). doi:[10.1029/2001JD000967](https://doi.org/10.1029/2001JD000967)
- Torres, A.L., Thompson, A.M.: Nitric oxide in the equatorial Pacific boundary layer: SAGA 3 measurements. *J. Geophys. Res.* **98**(D9), 16,949–16,954 (1993). doi:[10.1029/92JD01906](https://doi.org/10.1029/92JD01906)
- Vøgt, R., Crutzen, P.J., Sander, R.: A mechanism for halogen release from sea-salt aerosol in the remote marine boundary layer. *Nature* **383**, 327–330 (1996)
- von Glasow, R.: Atmospheric chemistry: sun, sea and ozone destruction. *Nature* **453**, 1195–1196 (2008)
- von Glasow, R., Sander, R., Bott, A., Crutzen, P.J.: Modeling halogen chemistry in the marine boundary layer 1. Cloud-free MBL. *J. Geophys. Res.* **107**(D17), 4341 (2002). doi:[10.1029/2001JD000942](https://doi.org/10.1029/2001JD000942)

- Watanabe, K., Nojiri, Y., Kariya, S.: Measurements of ozone concentrations on a commercial vessel in the marine boundary layer over the northern North Pacific Ocean. *J. Geophys. Res.* **110**, D11310 (2005). doi:[10.1029/2004JD005514](https://doi.org/10.1029/2004JD005514)
- Yang, X., Cox, R.A., Warwick, N.J., Pyle, J.A., Carver, G.D., O'Connor, F.M., Savage, N.H.: Tropospheric bromine chemistry and its impacts on ozone: a model study. *J. Geophys. Res.* **110**, D23311 (2005). doi:[10.1029/2005JD006244](https://doi.org/10.1029/2005JD006244)
- Yuter, S.E., et al.: Physical characterization of tropical oceanic convection observed in KWAJEX. *J. Appl. Meteorol.* **44**, 385–415 (2005)
- Zipser, E.J., Lutz, K.R.: The vertical profile of radar reflectivity of convective cells: a strong indicator of storm intensity and lightning probability? *Mon. Weather. Rev.* **122**, 1751–1759 (1994)